

Miniature Circularly Polarized Antenna for UHF RFID Handheld Reader: Design and Experiments

Le-Huy Trinh^{1, 2, 3, *}, Khai-Thong Lu², Manh-Thao Nguyen²,
Nguyen-Vu Truong³, and Fabien Ferrero⁴

Abstract—A low-profile circularly polarized (CP) antenna for a handheld Ultra-High Frequency Radio Frequency Identification (UHF RFID) reader is proposed in this paper. The radiating part on the top substrate is composed of three inverted-F elements rotated 120° around the center of the structure. A power splitting circuit, placed on the bottom substrate, based on a series transmission line feed delivers equal amplitude to the three IFAs with a sequential 120° phase shift. Both layers are fabricated on low-cost FR4 material. This design has a disk form factor with a compact size of 35 mm circle radius and an 8.6 mm height. The measurement shows good results with S_{11} as lower than -10 dB for the whole band, 3 dB-axial ratio around 110° (10 MHz of bandwidth), directivity reaching 4.4 dBic, and the total gain of the antenna is 1.9 dBic. In order to validate the proposed antenna performance, a UHF RFID handheld reader is built based on the ThingMagic M6E-Nano module. Different scenarios are investigated to validate the proposed antenna performance in a real environment.

1. INTRODUCTION

Ultra-High Frequency Radio Frequency Identification (UHF RFID) technology is expanding exponentially and is driving Industry 4.0 revolution [1]. With the advantage of fast reading rate and long-distance battery-less reading capability, UHF RFID is disrupting supply management chain, logistics application, and access control work. Several blocks are critical on an RFID reader system, and antenna is a key element to maximize reading performance. According to a brief review on UHF RFID antenna in the market [2], handheld devices usually use a ceramic patch antenna. Moreover, Circular Polarization (CP) is one of the critical characteristics of a UHF RFID antenna to enable tag reading regardless of their orientation. In addition to CP requirement, antenna size and efficiency must also be considered for handheld devices. Some studies about printed patch antenna [3, 4] performance in retail shelf multi-item detection are realized.

Recently, a new CP and directional antenna design has been proposed to replace wide-use patch antenna. That antenna design is usually more efficient and also maintains a compact size. A typical circularly polarized antenna design uses the sequentially rotating technique which includes a two-layer substrate with microstrip or coplanar waveguide on top [5]. The first layer is designed as a feeding network which delays signal phase and distributes even energy between ports. The second layer has multiple omnidirectional antennas which rotate a certain angle respectively to each other depending on the phase which has been delayed in the first layer. Another type of antenna design uses two crossed dipoles placed orthogonally to create 90° phase delay. Then CP radiation feature is generated [6].

Received 10 April 2020, Accepted 6 May 2020, Scheduled 1 June 2020

* Corresponding author: Le-Huy Trinh (Le-Huy Trinh).

¹ Graduate University of Science and Technology (GUST), VAST, Vietnam. ² Vietnam National University, Ho Chi Minh City, Vietnam. ³ Institute of Applied Mechanics and Informatics, VAST, Ho Chi Minh City, Vietnam. ⁴ University Cote d'Azur, LEAT/CNRS, France.

Many study efforts have been realized to create a low-profile antenna suitable for UHF RFID handheld reader with decent overall performance. In article [7], a compact size $45 \times 45 \times 9$ mm antenna is reported which consists of four meandered inverted F antennas and a series-feed power divider. This antenna achieves great performance with a gain of 2.2 dBic and a 3-dB gain beamwidth of 150° . By using 3D printing technology, [8] applies PLA material as the substrate to increase efficiency thank to low loss tangent. Notably, the antenna design is independent of standard thickness. Thus the antenna height is easily adjusted. This design shows the gain of 2dBic and the impedance bandwidth of 6 MHz (862–868 MHz). In paper [9], the antenna size is reduced by using a four-meandered-inverted-F structure, and a second radiating element used for WLAN 2.4 GHz application is added in the middle of the top layer. By using this design, the antenna will have dual-channel ability but with a downside as low directivity gain, which is only -0.6 dBic maximum for UHF RFID and 1.2 dBic for WLAN. Another structure is shown in [10] that combines a crossed dipole structure and rectangular metals to improve the impedance matching and also expand the axial ratio bandwidth. However, this concept has a limited ground plane. The antenna performance could be affected by cable length as well as objects placed behind.

In this paper, a low-profile circularly polarized antenna used for UHF RFID handheld reader is presented. The main objective is using FR4-Epoxy as the substrate material to reduce the fabrication cost. However, this FR4 Epoxy has a high dissipation factor (0.02) that is the reason for the decrease in antenna performance and gain. In order to limit this effect, the length of the feeding network needs to be reduced. In this case, the 3-way series-feed structure could be the right solution thanks to its short length compared to the conventional feeding network while maintaining the circularly polarized feature. Thanks to this proposal, by reducing the dimension of the feeding network, the losses caused by FR4 could be reduced. The combination of a 3-element structure with a 3-way series-feed power divider is studied and fabricated. Moreover, a UHF RFID is built for testing with several commercial tags that are placed at different orientations to validate the proposed antenna suitability for UHF RFID handheld application.

2. ANTENNA DESIGN

Existing solution based on quadri-filar design has shown promising results. However, the paper in [11] has studied and compared this structure with the tri-filar model. With the same delay lines concept, the 3-element feeding network will be simpler and have a lower loss because of the shorter line length. Thus, the main idea of this work is to focus on a tri-filar design in order to simplify and minimize feeding circuit losses that lead to the low-cost but high-loss substrate material.

The proposed antenna uses three identical inverted-F Antennas (IFAs) as radiating elements. Thanks to this structure, the antenna provides a more compact form than other antennas. Each element is rotated around the centre of the substrate 0° , 120° , and 240° , respectively. To optimize the length of the elements, inverted-F shape runs along on the edge of the top substrate and turns directly into the centre at the end. Feeding line and ground-short are placed at the beginning of each element, which connect with the feeding network at the bottom PCB via the copper wires, as shown in Fig. 1.

The second part of the antenna is the feeding network located on the bottom substrate. The structure overview of the feeding line is shown in Fig. 2. This layer is in charge of splitting the RF

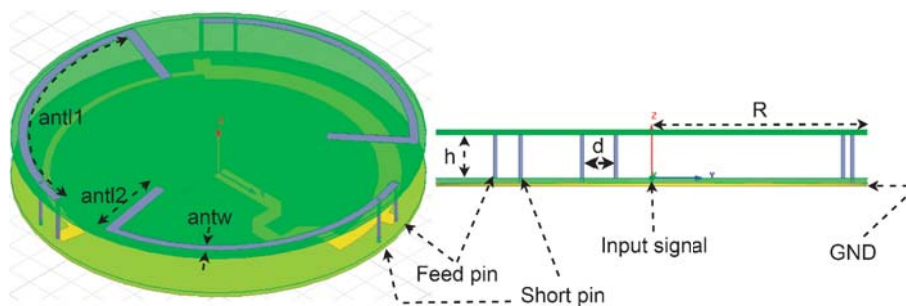


Figure 1. Overview of proposed antenna.

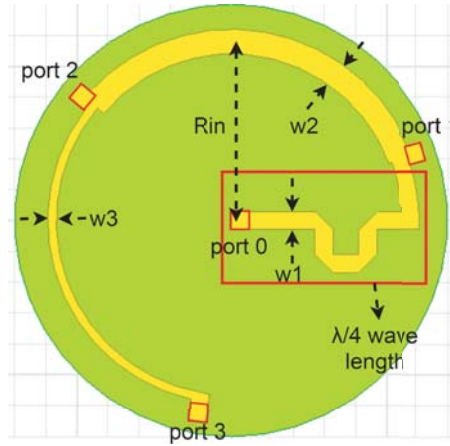


Figure 2. The series-feed power divider structure.

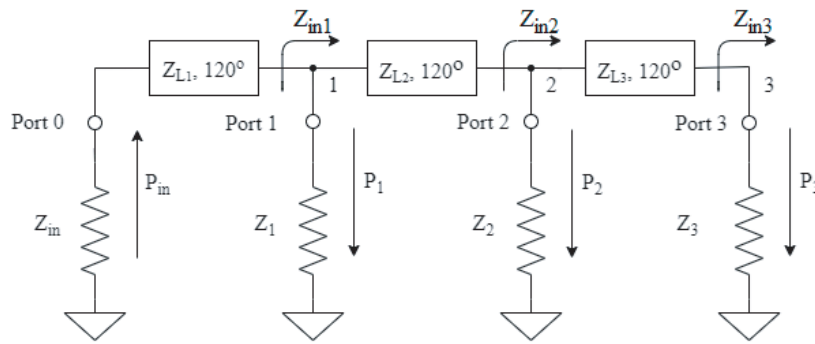


Figure 3. Equivalent circuit of series-feed power divider.

signals with the correct phase shift of 120° and equal magnitude at each port. In order to achieve these requirements, a traditional series-feed power divider (SFPD) is used in this proposed design. SFPD is a very simple and efficient structure which is popular in circularly polarized antenna design [12–16]. In order to focus on low-cost application, an FR4 Epoxy substrate is selected ($\epsilon_r = 4.4$, $\tan \delta = 0.02$). Despite higher losses than RF substrate, the permittivity of 4.4 is in a good range to provide a 120° phase shift between the ports.

Value of parameter R_{in} affects the delay-phase of each port. Values w_1 to w_3 affect the power distribution property. Moreover, a quarter-wave line that connects to the antenna primary port works as a phase shifter and also an impedance matching circuit. Based on the equation in article [16], the dimension of lines in the feeding network can be calculated. The equivalent circuit is depicted in Fig. 3 with Z_{in} , Z_1 , Z_2 , Z_3 being the impedance of the input (as port 0), port 1, port 2, and port 3, respectively. At this structure, these values are 50 Ohm. The proposed 3-way power divider provides three equal powers at the outputs of the circuit that satisfy the condition of

$$P_1 = P_2 = P_3 = \frac{P_{in}}{3} \quad (1)$$

The three output ports are connected through three one-third wave impedance transformers. These lines have Z_{L1} , Z_{L2} , Z_{L3} as the impedance and the phases of 120° . The input impedances Z_{in1} , Z_{in2} , and Z_{in3} at points 1, 2, and 3 can be obtained in Eq. (2)

$$Z_{in1} = Z_1 \frac{P_1}{P_{in}},$$

$$Z_{in2} = Z_2 \frac{P_2}{P_{in} - P_1},$$

$$Z_{in3} = Z_3. \quad (2)$$

Using Eqs. (1) and (2), the input impedance at each point can be obtained

$$Z_{in1} = \frac{Z_1}{3}, \quad Z_{in2} = \frac{Z_2}{2}, \quad Z_{in3} = Z_3. \quad (3)$$

Finally, the characteristic impedance of the transformer lines can be expressed as

$$\begin{aligned} Z_{L1} &= \sqrt{Z_{in} Z_{in1}}, \\ Z_{L2} &= \sqrt{\frac{Z_{in1} Z_{in2} Z_1}{Z_1 - Z_{in1}}}, \\ Z_{L3} &= \sqrt{\frac{Z_{in2} Z_{in3} Z_2}{Z_2 - Z_{in2}}}. \end{aligned} \quad (4)$$

In the proposed design, the impedances of the ports are the same as $Z_0 = 50 \Omega$. Thus, using Eqs. (3) and (4) the following equations can be obtained

$$\begin{aligned} Z_{L1} &= \frac{Z_0}{\sqrt{3}} = 28.86 \Omega, \\ Z_{L2} &= \frac{Z_0}{2} = 25 \Omega, \\ Z_{L3} &= Z_0 = 50 \Omega. \end{aligned} \quad (5)$$

By using the 3D EM solver, the feeding circuit that fits with the impedance in Eq. (5) is simulated. Fig. 4 shows the simulation result of S -parameters with the magnitudes in dB and the phases in degree. The power of each port is shown close to value -5 dB, which is one-third of the power from the input power. These results prove that the power divider operates properly as the above calculations. Moreover, the phase difference between the ports has a value close to 120° .

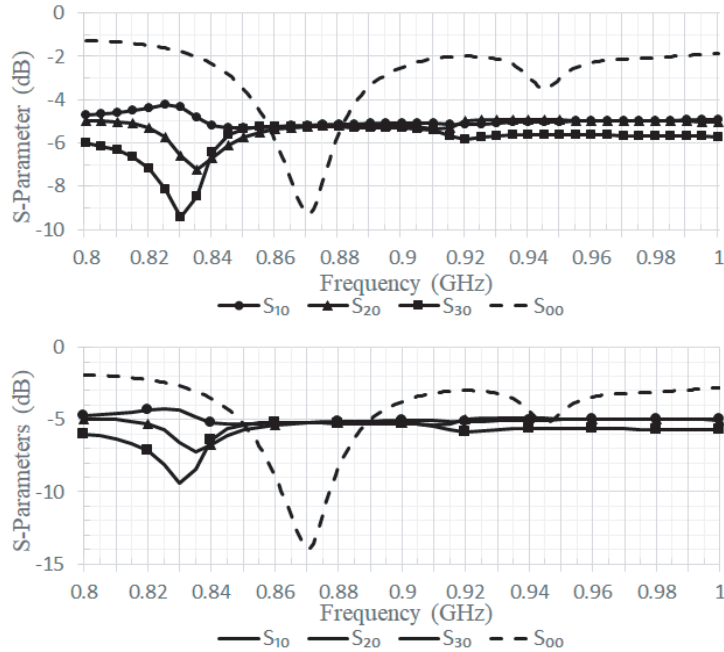


Figure 4. S parameter of proposed antenna.

3. ANTENNA FABRICATION AND MEASUREMENT

The proposed antenna is fabricated on a 0.8 mm thick FR4 Epoxy substrate with $\epsilon_r = 4.4$ and $\tan \delta = 0.02$. The antenna parameters are optimized by using a 3D EM solver and shown in Table 1. Besides, the top and bottom boards are connected by soldering copper wires. These wires have a length of 8.6 mm to ensure the space between the boards is exactly 7 mm. Finally, a standard female SMA is soldered at port 0 of the feeding circuit.

Table 1. Optimize parameter of the proposed antenna.

<i>w1</i>	<i>w2</i>	<i>w3</i>	<i>antl1</i>	<i>antl2</i>
3.5 mm	4 mm	1.4 mm	54.2 mm	15.5 mm
<i>antw</i>	<i>h</i>	<i>d</i>	<i>R</i>	<i>Rin</i>
2 mm	7 mm	9.5 mm	35 mm	29 mm

Figure 5 reports the measured and simulated reflection coefficients of the proposed antenna. The noticed discrepancies could come from the fabrication process. However, these result curves show a good agreement with each other. By measuring with the Starlab Satimo system, the antenna radiation at 870 MHz is determined and plotted in Fig. 6 which shows a maximum gain of 1.9 dBic and -3 dB beamwidth about 110° . Moreover, the measured realized gains are shown in Fig. 7. It can be seen that the antenna has a maximum efficiency of -2.8 dB at 870 MHz. However, compared to the simulation, these results are quite low due to the cable loss and the imperfection of the measurement system. Finally, the axial ratio in the main beam direction is presented in Fig. 8. The 3 dB axial ratio bandwidth is obtained of 10 MHz, which covers enough the UHF RFID band in ETSI Region.

A comparison with the state of art is summarized in Table 2. Firstly, the proposed antenna has the smallest dimension relative to wavelength among the references. Then, compared to [7] and [8], the peak gain of the proposed antenna is much lower because the losses come from the substrate. The $\tan \delta$ of the references are lower than FR4-Epoxy which is used in this article (0.002 and 0.007 versus 0.02). However, the antennas in [7] and [8] have narrow frequency bandwidths about 1.6% and 0.7%, respectively. Compared to the antenna using FR4-Epoxy as the substrate, the proposed design has the highest gain and adequate bandwidth which fully covers the UHF RFID frequency band. Finally, the results above show that the tri-fillar structure is very suitable for the antenna using the low-cost but high-loss substrate.

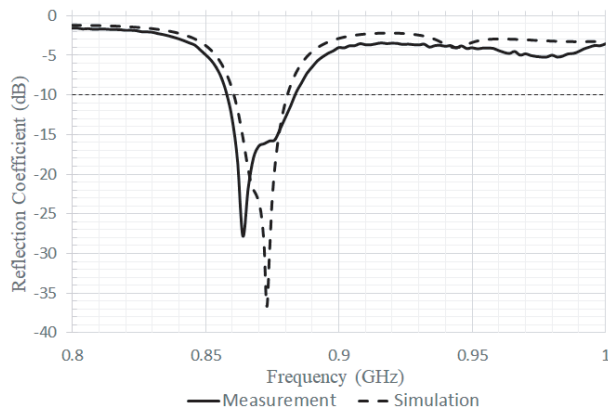


Figure 5. Simulated and measured reflection coefficient.

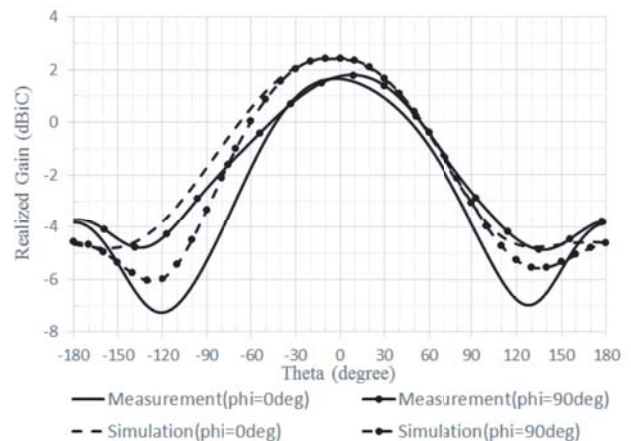


Figure 6. Simulated and measured gain at 870 MHz, $\phi = 0^\circ$ and $\phi = 90^\circ$.

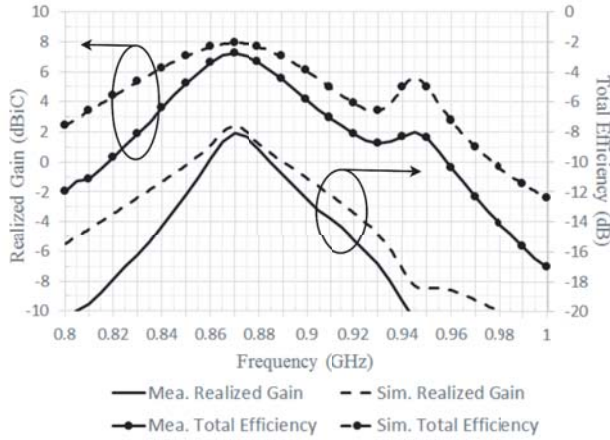


Figure 7. Simulated and measured gain and total efficiency versus frequency.

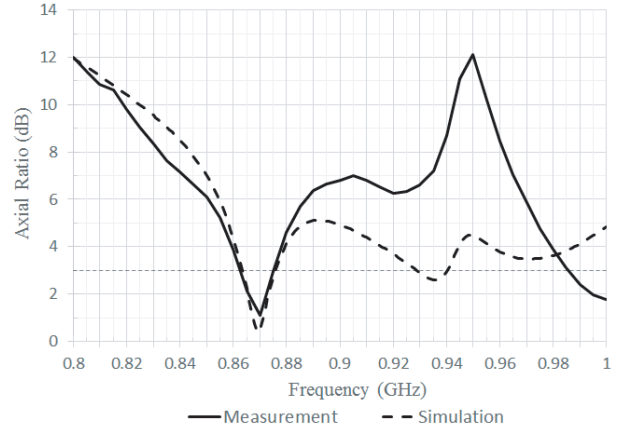


Figure 8. Simulated and measured axial ratio of the proposed antenna.

Table 2. Comparison of various CP UHF RFID reader antennas.

	[7]	[8]	[9]	[10]	Proposed Work
Max. Dimension*	0.2λ	0.24λ	0.26λ	0.26λ	0.2λ
Center Freq.	919 MHz	866.5 MHz	915 MHz	932 MHz	870 MHz
Substrate $\tan\delta$	0.002	0.007	0.02	0.02	0.02
Peak RHCP Gain	2.2 dBic	2 dBic	-0.6 dBic	1.4 dBic	1.9 dBic
Freq. Bandwidth	1.6%	0.7%	5.6%	11.8%	3%
-3 dB Beamwidth	150°	120°	N/A	80°	110°

* λ is the wavelength at the center frequency.

4. EXPERIMENTAL VALIDATION

To validate the performance of the proposed antenna, a testing scenario is realized as described in Fig. 9. The surrounding environment is an essential factor that affects the test result significantly. Therefore, some condition has been paid attention when setting up the testing places to ensure the accuracy of the measurement. The reader, antenna, and tags are located 45 cm higher from the ground to avoid Fresnel zone reflection. The tags are glued to a plastic box and situated in the same horizontal plane as the reader antenna. Thanks to a support object (a small paper box) which is arranged underneath the plastic card, the tag height could be adjusted. The distances between the reader and tags are 40 mm, 60 mm, 80 mm, 100 mm, and 120 mm, respectively. At each distance, the reader is set with the same configuration and launched within 10s. Finally, the tag read count (TRC) is recorded and processed.

At the other side, three types of tag with different dimensions and structures are used for measurements (Fig. 10). Table 3 shows the specification of these tags. With each tag, different positions are proposed. Firstly, the tag is located on the YOZ plane known as position 1, while position 2 is also on the same plane, but the tag is rotated clockwise. Then, in position 3, the tag is placed in the XOY plane.

The UHF RFID reader system used in this test is ThingMagic M6E-Nano with a maximum output power of +27 dBm. This module is compatible with the Gen-2 UHF RFID protocol. In order to maximize the number of tag reading times, the following configurations are set for M6E-Nano. The Backscatter Link Frequency (BLF) is 250 kHz, and the Type A Reference Interval (TARI) is 25 μ s. Both of these parameter values are default and also the only option in M6E-Nano. Miller2 is enabled to archive a faster data rate. Session 0 is used to decrease the tag responding time to a query from the

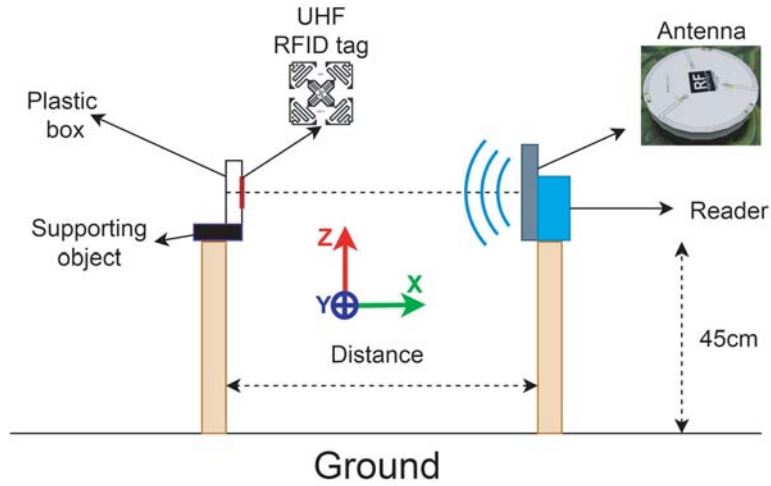


Figure 9. Experiment environment setup.

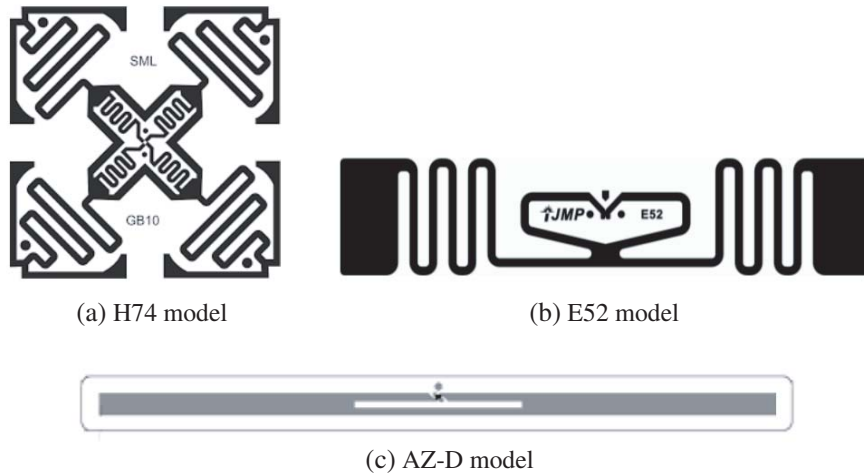


Figure 10. RFID tags used in experimental.

Table 3. Specification of the commercial passive tags.

Model	Antenna Design	Dimension	Chipset
H74	Dual-Dipole	50 mm × 50 mm	Monza 4D
E52	Tip Loading	73.5 mm × 21.2 mm	Monza 5
AZ-D	Straight Dipole	124 mm × 10 mm	Higgs 3

reader. Q is set to 0 for faster read rate, and target A & B are used to read all states of the tag. The prototype of this device is reported in Fig. 11.

A commercial CP patch antenna is used as the reference [17]. This CP patch antenna has a dimension of 260 × 260 mm, a very high gain of 8.3 dBic, and a wide 3-dB beamwidth of 65°. To validate the proposed antenna in real environment, the detectability score (DS) is used. This score is defined in Eq. (6).

$$DS_{Proposed Ant.} = TRC_{Proposed Ant.} / TRC_{ref[17]}. \tag{6}$$

where $DS_{Proposed Ant.}$ is the detectability scores of the proposed antenna. Then, $TRC_{ref[17]}$ and



Figure 11. The prototype of the UHF RFID handheld reader.

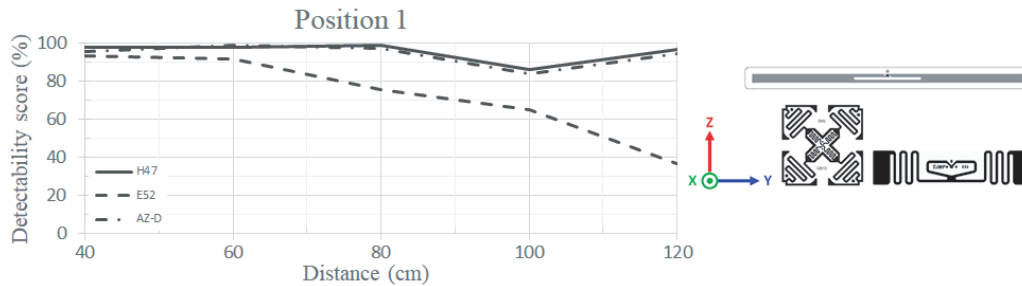


Figure 12. Measured detectability score of the tags at position 1.

$TRC_{Proposed Ant.}$ are the tag read counts of the antenna in [17] and the proposed antenna, respectively.

For the scenario that the tags are placed at position 1, the measured results are presented in Fig. 12. The tags H47 and AZ-D have shown a DS that maintains more than 80% (we measure the DS with different distances between reader and tag). With the small size, the E52 tag has shown a lower DS than other tags, and it decreases over the separation.

The measurement of the tags at position 2 is described in Fig. 13. Thanks to the symmetric structure, the score of H47 is almost unchanged. That could confirm the CP feature of the tag's antenna. By rotating the tags around the x -axis, the DS of AZ-D is quite changed. Instead of the score that is lower than 80% with the distance of 80 cm, the measurements of other ranges are always more than 80%. E52 is still the worst-performing tag among the RFID transponders. It will not be read if

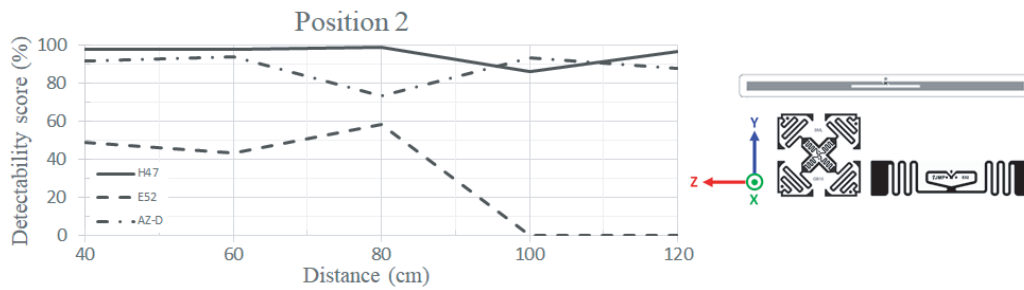


Figure 13. Measured detectability score of the tags at position 2.

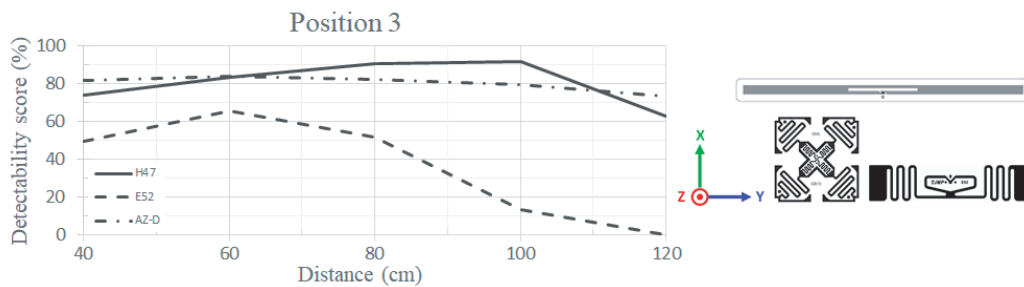


Figure 14. Measured detectability score of the tags at position 3.

the distance is more than 100 cm.

The last measurement is realized with position 3, and the results are reported in Fig. 14. In general, the obtained scores are lower than the results of other positions. However, the DSs of H47 and AZ-D are still acceptable and varied around 80%. According to the figure, the maximum read range of E52 tag is 120 cm. In summary, the measurement results show that thanks to the use of the proposed antenna at the reader, the influence of the tag orientation could be limited.

5. CONCLUSION

A circle-shape CP antenna with three-port rotating sequence and a series-feed power divider is designed and evaluated. The result has determined that this proposed antenna has reasonable performance compared to other antennas in the references. Notably, the tri-filar structure is proposed as a good candidate for the high-loss based material antenna. Finally, the antenna provides a frequency bandwidth that fully covers UHF RFID ETSI band with reasonable gain and adequate beamwidth.

ACKNOWLEDGMENT

This research is funded by Graduate University of Science and Technology under grant number GUST.STS.DT2017-TT01.

REFERENCES

1. Murofushi, R. and J. Tavares, "Towards fourth industrial revolution impact: Smart product based on RFID technology," *IEEE Instrum. Meas. Mag.*, Vol. 20, No. 2, 51–56, 2017.
2. Lau, P. Y., Q. Chu, and Y. Wu, "Review on UHF RFID antennas," *2017 International Workshop on Electromagnetics: Applications and Student Innovation Competition*, 53–55, London, 2017.
3. Xiao, G., et al., "Printed UHF RFID reader antennas for potential retail applications," *IEEE Journal of Radio Frequency Identification*, Vol. 2, No. 1, 31–37, Mar. 2018.

4. Farhat, H., P. Iliev, P. Marriage, and N. Rolland, "An added value alternative to RAIN RFID items characterization in retail," *IEEE Access*, Vol. 6, 32430–32439, 2018.
5. Hall, P. S., J. S. Dahele, and J. R. James, "Eesign principles of sequentially fed, wide bandwidth, circularly polarised microstrip antennas," *IEE Proceedings H — Microwaves, Antennas and Propagation*, Vol. 136, No. 5, 381–389, Oct. 1989.
6. Bolster, M. F., "A new type of circular polarizer using crossed dipoles," *IRE Transactions on Microwave Theory and Techniques*, Vol. 9, No. 5, 385–388, Sep. 1961.
7. Bang, J., C. Bat-Ochir, H. Koh, E. Cha, and B. Ahn, "A small and lightweight antenna for handheld RFID reader applications," *IEEE Antennas and Wireless Propagation Letters*, Vol. 11, 1076–1079, 2012.
8. Colella, R., L. Catarinucci, A. Michel, and P. Nepa, "Design of a 3D-printed circularly polarized antenna for portable UHF RFID readers," *2017 IEEE International Conference on RFID Technology and Application (RFID-TA)*, 225–228, Warsaw, 2017.
9. Caso, R., A. Michel, M. Rodriguez-Pino, and P. Nepa, "Dual-band UHF-RFID/WLAN circularly polarized antenna for portable RFID readers," *IEEE Transactions on Antennas and Propagation*, Vol. 62, No. 5, 2822–2826, May 2014.
10. Lin, Y., Y. Wang, H. Chen, and Z. Yang, "Circularly polarized crossed dipole antenna with phase delay lines for RFID handheld reader," *IEEE Transactions on Antennas and Propagation*, Vol. 60, No. 3, 1221–1227, Mar. 2012.
11. Ferrero, F., L. H. Trinh, T. Telkamp, and R. Spurett, "Low cost compact terrestrial antenna for space LPWAN communication," *40th ESA Antenna Workshop Antenna Developments for Terrestrial and Small-Space Platforms (ESA-ESTEC 2019)*, Noordwijk, Netherlands, ESA, Oct. 2019.
12. Xu, P., Z.-H. Yan, T.-L. Zhang, and X.-Q. Yang, "Broadband circularly polarized slot antenna array using a compact sequential-phase feeding network," *Progress In Electromagnetics Research C*, Vol. 47, 173–179, 2014.
13. Chen, X., L. Yang, J. Zhao, and G. Fu, "High-efficiency compact circularly polarized microstrip antenna with wide beamwidth for airborne communication," *IEEE Antennas and Wireless Propagation Letters*, Vol. 15, 1518–1521, 2016.
14. Inserra, D., W. Hu, and G. Wen, "Design of a microstrip series power divider for sequentially rotated nonuniform antenna array," *International Journal of Antennas and Propagation*, 1–8, 2017.
15. Piroutiniya, A., M. H. Rasekhmanesh, and P. Mohammadi, "Wide-band circularly polarised antenna array using sequential phase feed structure and reinforced square radiating patch element," *IET Microwaves, Antennas and Propagation*, Vol. 12, No. 8, 1395–1399, Apr. 7, 2018.
16. Reddy Sura, P. and S. N. Reddy, "Broad band CP antenna array for X-band applications using sequential phase rotation technique," *Optik*, Vol. 203, 163547, 2020.
17. FEIG Electronic GmbH, "UHF antenna ID ISC.ANT.U250/250-EU/-FCC," Nov. 4, 2011, [Online]. Accessed on: Mar. 4, 2020.